ADVANCED QUANTUM TECHNOLOGIES
www.advquantumtech.com

Tailoring Fano Lineshape in Photonic Local Density of States by Losses Engineering

Nicoletta Granchi and Massimo Gurioli*

Non-Hermitian theory in photonics revolutionized the understanding of optical resonators, thanks to the concept of quasi-normal modes (QNM) and to a deep revision of the Purcell factor expression. Counterintuitive effects followed, such as complex modal volumes and non-Lorentzian local density of states (LDOS) of QNMs. One of the fascinating aspects of non-Hermitian theory is the analogy with quantum mechanics for autoionizing electronic levels where the absorption cross'section is characterized by Fano lineshapes, caused by interference between the probability of absorption in the continuum and in the bound states. In photonics Fano lineshapes can arise from QNM normalization through the complex modal volume. The link between Fano lineshapes in photonic LDOS of QNMs and in the case of autoionizing states needs to be clarified. Here, by developing an analytical model based on the role of losses in the QNM normalization, they clarify the meaning of the phase of QNM normalized fields (*q*Fano parameter),linking QNMs normalization to the concept of interference among the resonant and the leaky modes. This inspired the design of photonic crystal (PhC) cavity that exhibits LDOS with Fano character inside the itself, providing a proof of principle on how to mold the radiative lifetime by Purcell effect.

1. Introduction

PhC cavities are nowadays the state-of-the-art devices for light confinement at the nanoscale and are largely employed to enhance the radiative decay rate via Purcell effect, in view of developing devices based on efficient quantum sources. In addition, they are basic elements in many fields of research ranging from integrated photonics,[1] optical,[2] and sensing[3,4] to quantum electrodynamics,[5] and topological photonics.[6] At the basis of the control of the Purcell effect[7] is the comprehension and study of two physical quantities: the Q factor and the modal volume V of the cavity. For these reasons, many successful examples in which the Q factor is controlled and optimized both theoretically and experimentally[8–13] can be brought up. The concept of modal volume, which is less intuitive than the Q factor since it is a function of the position inside the cavity, has been recently clarified by introducing its unavoidable complex-valued nature based on the non-Hermitianicity of open systems.[14–18] Non-Hermitian theory in photonics has imposed a major breakthrough in the understanding of optical micro- and nano-resonators and their applications, thanks to the physical insight provided by the underlying concept of their natural resonances, the QNMs.[15,16,19] Indeed, rapid progress in photonics has brought many examples of resonant optical phenomena associated with the physics of Fano resonances.[20] A major interest in the study of photonic Fano resonances lies in the sharp transmission-reflection curves supplied by their typical lineshapes displaying a sharp transition from total transmission to total reflection, which makes them appealing for optical switching and sensing applications.[21–24]

One of the fascinating aspects at the basis of non-Hermitian theory is the analogy with quantum mechanics for autoionizing electronic levels where the absorption cross section exhibits Fano lineshape.[25] Following the description of Ugo Fano, "interference between the direct and indirect photo-ionizations becomes then constructive on one side of the line center (resonance point) and destructive on the other", leading to the asymmetric Fano absorption profile. Indeed, the Fano resonance occurs when a discrete quantum state interferes with a continuum band of states, and it arises with an intensity F expressed as a function of energy E which is well reproduced by the formula:[20,26,27]

$$F\ (E) = C_0 + F_0 \frac{\left[q + 2\left(E - E_0\right)/\Gamma\right]^2}{1 + \left[2\left(E - E_0\right)/\Gamma\right]^2} \tag{1}$$

where C_0, F_0 are amplitude factors, E_0 and Γ are the resonant energy and width, while the dimensionless factor q, i.e., the Fano parameter, accounts for the line-shape asymmetry; for example, the lineshape is Lorentzian if $q \to \pm\infty$, quasi-Lorentzian (dip) if $q = 0$, and it is anti-symmetric if $q \approx \pm 1$ (pure Fano).

In quantum mechanics the common picture predicts that Fano resonances are related to the interference between the probability amplitudes of absorption in the continuum states and the one of absorption in the bound states. On the contrary, the introduction of the complex modal volume arising from QNM normalization in non-Hermitian theories has unveiled contributions with Fano

N. Granchi, M. Gurioli
Department of Physics and Astronomy
University of Florence
Sesto Fiorentino 50019, Italy
E-mail: granchi@lens.unifi.it

The ORCID identification number(s) for the author(s) of this article can be found under https://doi.org/10.1002/qute.202300199

DOI: 10.1002/qute.202300199

lineshapes to the photonic LDOS.[14] Despite the fact that any photonic resonator can be considered a bound state embedded in the continuum,[28] that is the analogous of atomic autoionizing states, the link between the Fano lineshapes in photonic QNMs and electronic absorption in autoionizing states still needs to be fully clarified.

Here, by developing a simple, yet effective analytical model based on the role of leaky modes in the QNM normalization and by designing and simulating the photonic LDOS in a modified L3 photonic cavity on slab, we shed light on the meaning of the phase of QNM normalized fields (i.e., the q Fano parameter), establishing a link between QNMs normalization and the concept of interference among the resonant and the leaky modes. In particular, although these two aspects lead to the same result, i.e., the physical origin of Fano lineshapes in the photonic LDOS, this point has not been highlighted yet in the literature. Our simple model, based on both concepts, aims at finding this link. It indeed clarifies the interplay between resonant and leaky modes and helps in understanding important features in sight of tailoring the Fano LDOS. The results are carefully supported by Finite Element Method (FEM) and Finite Difference Time Domain (FDTD) simulations. The results obtained on the well-known L3 photonic crystal cavity suggest that the Fano parameter q is strongly dependent on the position inside the photonic system at the nanoscale; therefore, even in the case of an "isolated" QNM, the LDOS does not have an unique lineshape. However, an LDOS with Fano profile can only be found outside the cavity itself, even in the case of very small Q factors determined by large in-plane losses. Here we present the design of an engineered L3 which exhibits an LDOS with Fano character inside the cavity itself, showing as a proof of principle that it might be possible to tailor the Purcell radiative lifetime[7] of an emitter in resonance with the QNM by engineering the LDOS. Fano lineshapes with different degrees of asymmetry can be obtained within the same cavity for similar values of the Q-factor, showing that Fano asymmetry can be tailored in moderately lossy systems.

2. Results and Discussion

2.1. QNM Normalization and Fano Lineshapes

The theoretical framework of the analytical model here developed considers a quantum emitter with dipole moment $\mathbf{p} = p\mathbf{u}$, with $\mathbf{u}$ the dipole direction, at position $\mathbf{r}$ embedded in a photonic cavity. Within QNM theory, it is described by a set of modes with normalized electric fields $\tilde{\boldsymbol{E}}_n(\mathbf{r})$ and complex frequencies $\tilde{\omega}_n = \omega_n - i\Gamma_n$, with ω_n the resonant frequency and Γ_n the coherence damping rate.[15] It has been shown that the spontaneous emission rate $\gamma(\mathbf{r},\omega)$ (which is proportional to $\rho(\mathbf{r},\omega)$, the photonic LDOS) can be written as $\gamma\ (\mathbf{r},\omega) = \sum_n \gamma_n(\mathbf{r},\omega)$, where γ_n is the contribution of the n-th mode to γ, and is given by:[17]

$$\gamma_n\ (\mathbf{r},\omega) = \frac{2}{\hbar\varepsilon_0\varepsilon_r\,(\mathbf{r})}\,|\mathbf{p}|^2\,\frac{Q_n}{\left|\tilde{V}_n\,(\mathbf{r})\right|}\,\frac{\omega}{\omega_n} \times\left[\frac{\Gamma_n}{\left(q_n(\mathbf{r})^2+1\right)}\,\frac{\left(q_n(\mathbf{r})^2-1\right)\Gamma_n+2q_n\,(\mathbf{r})\,(\omega-\omega_n)}{(\omega-\omega_n)^2+\Gamma_n^2}\right] \tag{2}$$

where the complex-valued modal volume $\tilde{V}_n(\mathbf{r}) = [2\varepsilon_o\varepsilon(\mathbf{r})(\tilde{\boldsymbol{E}}_n(\mathbf{r})\cdot\mathbf{u})^2]^{-1}$ has been introduced in addition to $Q_n = \frac{1}{2}\omega_n/\Gamma_n$.[12] Equation (2) shows that the LDOS lineshape is a Fano profile through all modal contributions, with the Fano parameter $q_n\ (\mathbf{r}) = -\mathrm{Re}[(\tilde{\boldsymbol{E}}_n(\mathbf{r})\cdot\mathbf{u})]/\mathrm{Im}[(\tilde{\boldsymbol{E}}_n(\mathbf{r})\cdot\mathbf{u})]$ being associated to the spatial phase of the n-th QNM, which is a physical observable fully defined by the normalization. It is worth remembering that for large $q_n(\mathbf{r})$, that is for $\mathrm{Re}[(\tilde{\boldsymbol{E}}_n(\mathbf{r})\cdot\mathbf{u})] \gg \mathrm{Im}[(\tilde{\boldsymbol{E}}_n(\mathbf{r})\cdot\mathbf{u})]$ the lineshape is Lorentzian. To have a Fano profiles with strong asymmetric tails the condition $\mathrm{Re}[(\tilde{\boldsymbol{E}}_n(\mathbf{r})\cdot\mathbf{u})] \approx \mathrm{Im}[(\tilde{\boldsymbol{E}}_n(\mathbf{r})\cdot\mathbf{u})]$ is needed. At the same time, since in photonic crystal cavities both the real and imaginary part of $\mathrm{Re}[(\tilde{\boldsymbol{E}}_n(\mathbf{r})\cdot\mathbf{u})]$ oscillate at the nanoscale, Equation (2) predicts a spatial modulation of the LDOS lineshape for any QNM. However, having the condition of $\mathrm{Re}[(\tilde{\boldsymbol{E}}_n(\mathbf{r})\cdot\mathbf{u})] \approx \mathrm{Im}[(\tilde{\boldsymbol{E}}_n(\mathbf{r})\cdot\mathbf{u})]$ inside the cavity and for points of large value of $1/|\tilde{V}_n(\mathbf{r})|$, Fano profiles can only occur for extremely lossy QNM, such as in plasmonic resonances.

FEM simulations were performed on an L3 cavity on a slab,[8,29] embedded in a 2D PhC of different spatial footprints, i.e., different number of rows R of holes (highlighted in different colors from $R = 1$ to $R = 7$), as sketched in the left inset of **Figure 1**a.

The PhC consists in a system of air holes of radius 89 nm arranged with lattice constant 320 nm on a Silicon slab 220 nm thick. We calculate the solutions to the eigenvalue problem for each R, evaluating the complex eigenfrequencies $\tilde{\omega}_n = \omega_n - i\Gamma_n$, from which the Q-factor of the n-th mode is found as $Q = \omega_n/2\Gamma_n$. The values of Q of the L3 ground state are reported in Figure 1a as a function of R. The real and imaginary parts of the normalized field component Ey were calculated and normalized through the so-called Perfectly Matched Layer (PML) normalization[15] (see Experimental Section for details). Then, in the same graph of Figure 1a, Re[Ey] and 10xIm[Ey], were reported as a function of R after being normalized to the maximum to be compared with the trend of the quality factors. We observe that while Q and Re[Ey] decrease for smaller R, Im[Ey] increases. Therefore the increase of losses determines a large decrease of the Fano parameters as expected; however, even for Q-factors as small as $Q = 20$, at the center of the cavity we find $\mathrm{Re}[(\tilde{\boldsymbol{E}}_n(\mathbf{r})\cdot\mathbf{u})] \approx 10\ \mathrm{Im}[(\tilde{\boldsymbol{E}}_n(\mathbf{r})\cdot\mathbf{u})]$, that is still the condition that gives an almost Lorentzian profile in the photonic LDOS. It follows that reducing the Q is not a sufficient condition to have a pronounced Fano lineshape in the photonic LDOS.

It is important to consider that just like in the case of autoionizing electronic states,[25] a major role of the hybridization between the continuum of leaky modes and the quasi stationary waves is expected also in photonics. At first glance this feature is not observed in the results of Figure 1b, in which we report the FEM spatial distribution of Re[Ey] for the case of the L3 with $R = 6$, $Q = 4000$ (left panel) and with $R = 4$, $Q = 600$ (right panel), since the two maps are almost identical. However, by saturating the colors for large fields (Figure 1c), it is clear that the field at the periphery of the cavity is much larger for the case with $R = 4$. This is a clear signature of the increasing hybridization of the QNM with the leaky modes as a consequence of increasing the mode losses.

This picture led to the development of a simplified perturbation approach to the problem of QNM, with the only scope to highlight how normalization is linked to the interference between continuum and bound states to generate Fano profiles.

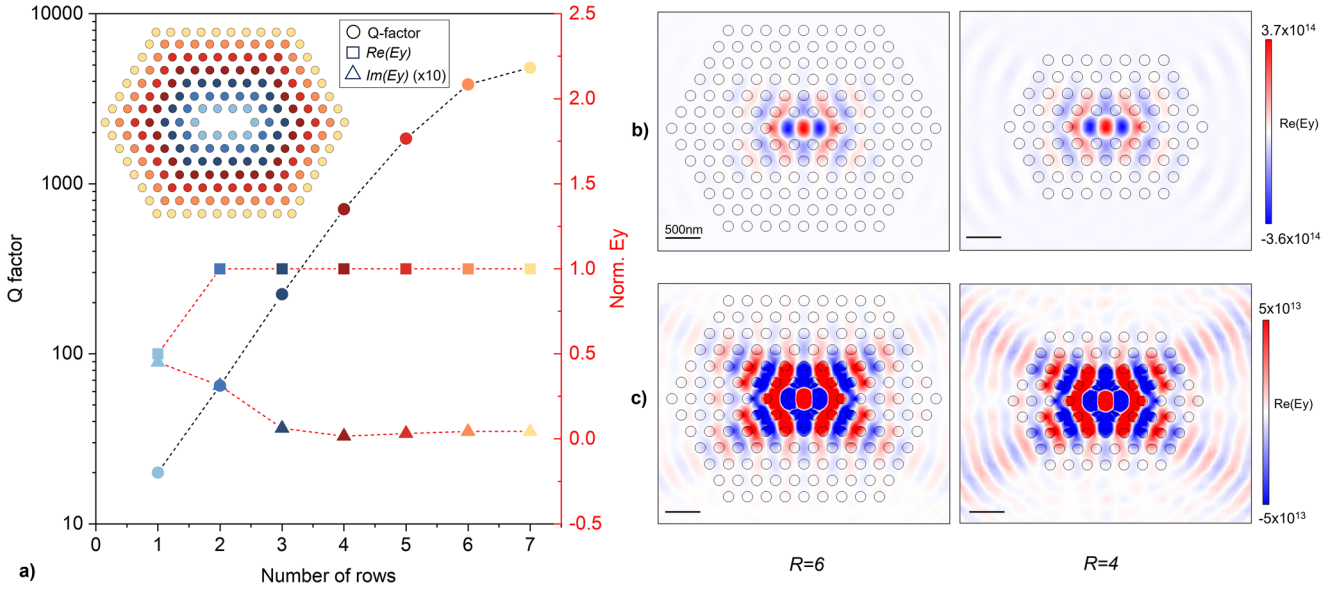

Figure 1. a) Dots: *Q*-factors of the L3 ground state reported as a function of the number of photonic crystal rows, *R*. Squares and triangles: corresponding values of Re[Ey] and 10xIm[Ey] for the L3 ground state as a function of *R*. b) FEM spatial profiles of Re[Ey] for the L3 with $R = 6$ (left) and $R = 4$ (right). c) FEM spatial profiles in saturated colorscale of Re[Ey] for the L3 with $R = 6$ (left) and $R = 4$ (right).

Let the QNM of an isolated cavity be described by the normalized electric field $\tilde{\boldsymbol{E}}_B(\mathbf{r})$.[14] In a non-magnetic and lossless dielectric system the normalization condition can be rewritten as:

$$\iiint \left(2\varepsilon_o \varepsilon\,(\mathbf{r})\,\tilde{\boldsymbol{E}}_B(\mathbf{r})^2\right) d^3\mathbf{r} = 1 \tag{3}$$

If the Q of the QNM is large, like for $R = 7$ and $Q = 4000$, then $\tilde{\boldsymbol{E}}_B(\mathbf{r})$ is almost real and the LDOS has a Lorentzian shape. Let this be called a bound state and assume that $\tilde{\boldsymbol{E}}_B(\mathbf{r})$ is indeed real (the suffix "*B*" means "bound"). As shown in Figure 1a, if the in-plane losses are increased by cutting the 2D PhC, then Q becomes quite small, like for example it is for $R = 4$ and $Q = 600$, and the electric field tends to spread out of the cavity. Also the field of this lossy cavity $\tilde{\boldsymbol{E}}_{QB}(\mathbf{r})$ (the suffix "Q*B*" means "quasi-bound") can be normalized:

$$\iiint \left(2\varepsilon_o \varepsilon\,(\mathbf{r})\,\tilde{\boldsymbol{E}}_{QB}(\mathbf{r})^2\right) d^3\mathbf{r} = 1 \tag{4}$$

We model this by assuming that the QNM field $\tilde{\boldsymbol{E}}_{QB}(\mathbf{r})$ in a lossy cavity can be expressed in terms of contribution of from the initial bound state $\tilde{\boldsymbol{E}}_B(\mathbf{r})$ and the "the continuum" of the leaky modes propagating out of the cavity$\tilde{\mathbf{E}}_C(\mathbf{r})$. Then:

$$\tilde{\boldsymbol{E}}_{QB}\ (\mathbf{r}) = a\tilde{\boldsymbol{E}}_B\,(\mathbf{r}) + b\tilde{\boldsymbol{E}}_C\,(\mathbf{r}) \tag{5}$$

Notably, Equation (5) means that the QNM in a lossy cavity can be described as a "hybridization" between the bound state $\tilde{\boldsymbol{E}}_B(\mathbf{r})$ and the continuum $\tilde{\boldsymbol{E}}_C(\mathbf{r})$ with a and b relative amplitudes.

We also assume that $\tilde{\boldsymbol{E}}_C(\mathbf{r})$ can be normalized:

$$\iiint \left(2\varepsilon_o \varepsilon\,(\mathbf{r})\,\tilde{\boldsymbol{E}}_c(\mathbf{r})^2\right) d^3\mathbf{r} = 1 \tag{6}$$

Then, from all normalization conditions, the following relation holds:

$$a^2 + b^2 + 2abC = 1 \tag{7}$$

where the field overlap integral $C = \iiint (2\varepsilon_o \varepsilon(\mathbf{r})\tilde{\boldsymbol{E}}_B(\mathbf{r}) \cdot \tilde{\boldsymbol{E}}_C(\mathbf{r}))d^3\mathbf{r}$ has been introduced. Hence, since $\tilde{\boldsymbol{E}}_C(\mathbf{r})$ is a continuum state, it is complex, and then also C is complex, even in $\tilde{\boldsymbol{E}}_B(\mathbf{r})$ is real.

If the contribution of the continuum to the "quasi-bound state" is not very large (i.e., $a \gg b$), within a perturbation theory approach we have to the first order in b that $a \approx 1 - bC$. Then:

$$\tilde{\boldsymbol{E}}_{QB}\ (\mathbf{r}) = (1 - bC)\,\tilde{\boldsymbol{E}}_B\,(\mathbf{r}) + b\tilde{\boldsymbol{E}}_C\,(\mathbf{r}) \tag{8}$$

Therefore, starting from a high Q cavity and increasing its losses, this equation states that the imaginary part of the field of the QNM of the lossy cavity comes from the overlap integral with the continuum C describing the leaky modes entering inside the cavity region. Finally, since the field $\tilde{\boldsymbol{E}}_{QB}(\mathbf{r})$ is complex, through Equation (2) the Fano profile in the photonic LDOS can be linked to the hybridization between the "original" bound state and the continuum, which is the essence of the Fano theory in quantum mechanics.

In particular, we can calculate the Fano parameter of the QB state q_{QB}, which is given by:

$$q_{QB}\ (\mathbf{r}) = -\frac{\mathrm{Re}\left[\left(\tilde{\boldsymbol{E}}_{QB}\,(\mathbf{r}) \cdot \mathbf{u}\right)\right]}{\mathrm{Im}\left[\left(\tilde{\boldsymbol{E}}_{QB}\,(\mathbf{r}) \cdot \mathbf{u}\right)\right]} \approx \frac{1}{\mathrm{Im}\,[bC] - \frac{\mathrm{Im}\left[b\left(\tilde{\boldsymbol{E}}_C(\mathbf{r}) \cdot \mathbf{u}\right)\right]}{\left(\tilde{\boldsymbol{E}}_B(\mathbf{r}) \cdot \mathbf{u}\right)}} \tag{9}$$

It is now clear that the dependance of $q_{QB}(\mathbf{r})$ on the point inside the photonic system reflects the change of weights of the contribution of the bound state $\tilde{\boldsymbol{E}}_B(\mathbf{r})$ and the continuum states $\tilde{\boldsymbol{E}}_C(\mathbf{r})$. It is expectable that by moving the position of the emitter

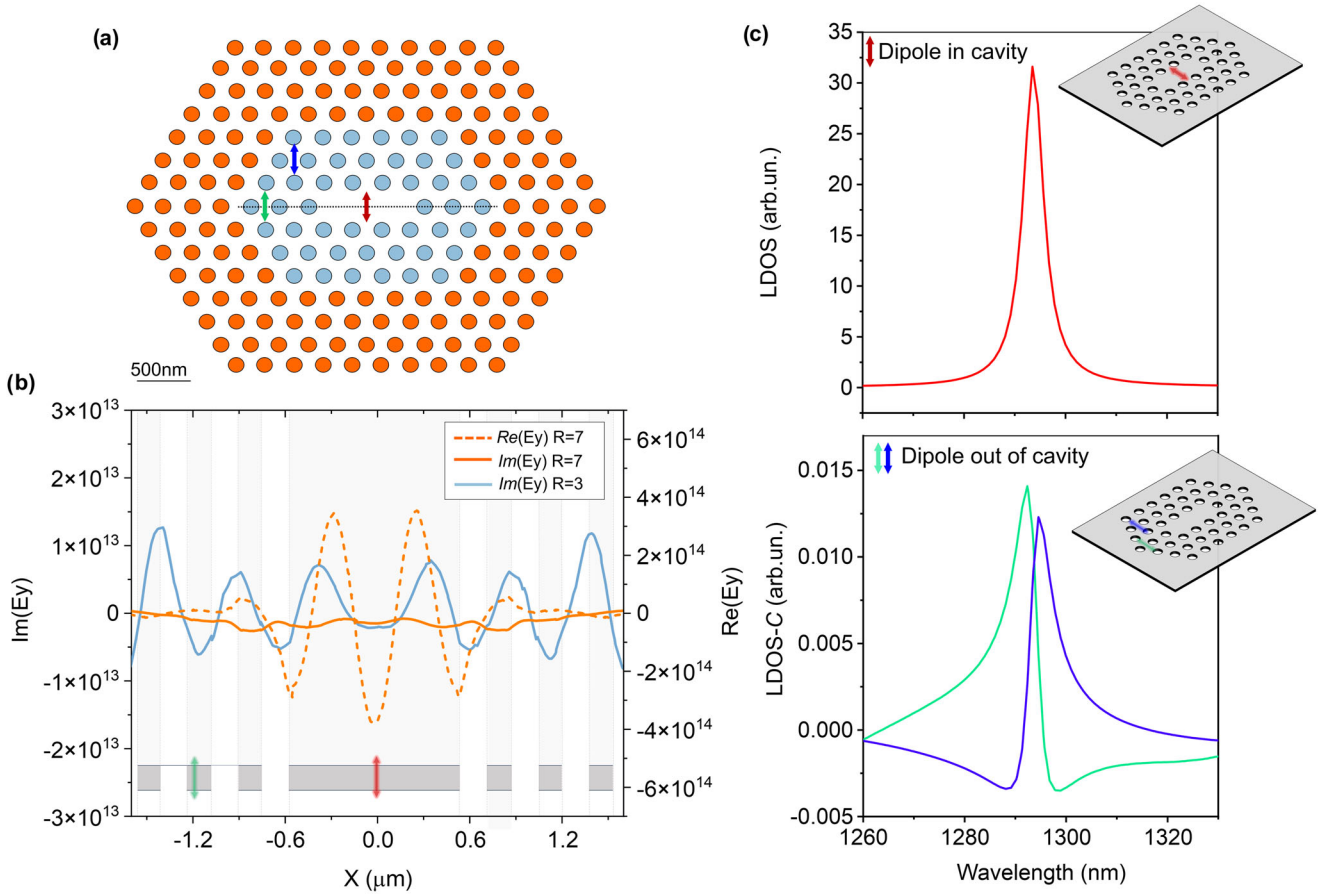

Figure 2. a) Sketch of the cavity with $R = 7$ (orange) and $R = 3$ (blue). The arrows indicate the positions of the dipoles in which the spectra are calculated. b) Spatial cuts of Im[Ey] (orange continuous line) and Re[Ey] (orange dashed line) along the black dashed line in a for the L3 with $R = 7$, compared with Im[Ey] for $R = 3$ (blue line). Overlapped to the cuts is the indication of the dielectric matrix (grey for Silicon and white for air holes). c) Upper panel: LDOS spectrum for the L3 with $R = 3$, calculated by positioning the dipole in the center of the cavity as highlighted by the red arrow. Bottom panel: Fano resonant contributions to the photonic LDOS obtained by subtracting from the total LDOS the baseline corresponding to the contribution from the continuum. Note that in any case and for any wavelengths the total LDOS is always positive. In the panel we plot the resonant LDOS in two positions out of the cavity (green arrow and dark blue arrow highlighting the dipole positions, which are reported in Figure 2b).

out of the cavity, where the ratio $\tilde{\boldsymbol{E}}_C(\mathbf{r})/\tilde{\boldsymbol{E}}_B(\mathbf{r})$ becomes large because of the contribution of the continuum, the Fano parameter of the LDOS $q_{QB}(\mathbf{r})$ will be small enough to observe asymmetric Fano profiles and will change at the nanoscale following the modulation of $\tilde{\boldsymbol{E}}_B(\mathbf{r})$.

The picture emerging from this simple model clarifies the results of FEM simulations reported in **Figure 2**, where we consider the L3 cavity with $R = 7$ (i.e., the high Q cavity) and with $R = 3$ (i.e., the lossy cavity); the sketches of the cavities are shown in orange blue in Figure 2a.

In Figure 2b we report for both cavities the spatial cuts of Im[Ey] (orange and blue continuous line for $R = 7$ and for $R = 3$) and Re[Ey] (orange dashed line for $R = 7$ and for $R = 3$ since they almost coincides) along the black dashed line in Figure 2a. Overlapped to the cuts is the indication of the dielectric matrix (grey for Silicon and white for air holes). Notably, the spatial cut of Im[Ey] for $R = 7$, highlights how in every x-coordinate the imaginary part of the field for $R = 3$ (blue) is bigger than the one for $R = 7$ (orange). This indicates that the L3 cavity with $R = 3$ exhibits a large contribution from the continuum. We then calculate through FDTD simulations the LDOS in three different positions of the exciting dipole (see section Methods for details): 1) Dipole placed at the center of the cavity, indicated by the red arrow in Figure 2b,c and 2) Dipole inside the PhC along the horizontal cut, with position indicated by the green arrow in Figure 2a,b. 3) Dipole inside the PhC along the lossy direction among the 30.7° diagonal, with position indicated by the dark blue arrow in Figure 2a. The results are shown respectively in the upper (dipole inside the cavity) and lower panels (dipole in the photonic crystal in two positions) of Figure 2c; we can observe that while the LDOS at the center has a Lorentzian lineshape, as the dipole is moved away from the cavity, the spectrum changes into a Fano lineshape with q parameter, extracted from fit, that changes from −2.6 to 1.8 as the dipole moves from the horizontal (green spectrum) to the diagonal line (dark blue spectrum). Note that these plotted Fano lineshapes represent the resonant contribution, since they have been obtained by subtracting from the LDOS the baseline corresponding to the contribution from the continuum

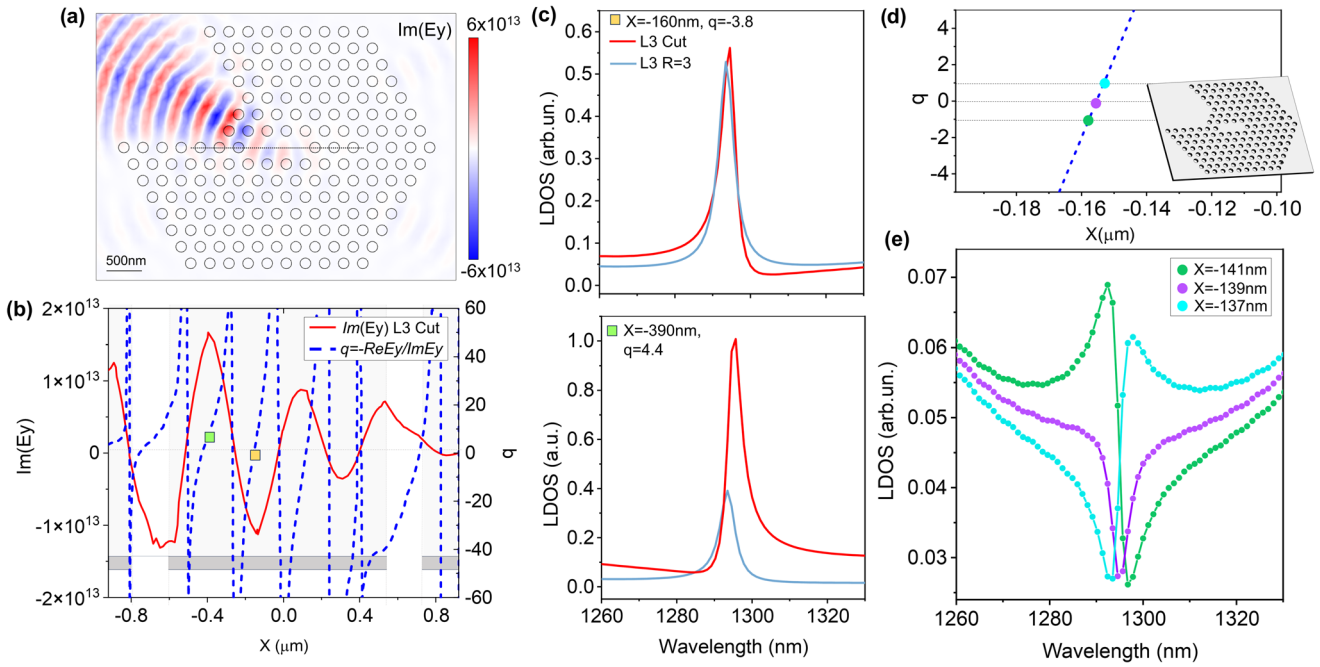

Figure 3. a) Im[Ey] of the cut L3 ground state. b) Spatial cuts of Im[Ey]) of the engineered cavity (red line) and profile of $q = -\mathrm{Re[Ey]}/\mathrm{Im[Ey]}$ (blue dashed line). c) Comparison between the LDOS of the cut L3 (red spectra) and the L3 with $R = 3$ (light-blue spectra) calculated near the center of the cavities x = −160 nm and inside the cavity at x = −390 nm (yellow and green squares). d) Zoom of the plot of q within 100 nm range. The green, purple, and cyan dot highlights the three positions in which the LDOS shown in (e) are calculated, which correspond to $q \approx -1$, $q \approx 0$, and $q \approx 1$.

(see Equation (1)). As suggested by the simple model, outside the cavity the hybridization of the QNM with the leaky modes increases, and therefore contributes to reveal the Fano profile. Indeed, in order to observe a Fano profile inside a PhC cavity, and not only at the borders, a large contribution of the continuum is needed. In standard photonic cavities, this could likely happen only for Q as small as few tens like in the plasmonic resonances.

2.2. Tailored Fano Lineshapes in Engineered Photonic Crystal Cavities

We now show how, by engineering the losses, it is possible to enhance the imaginary part of the QNM such that a Fano LDOS is displayed inside the cavity without decreasing too much the Q – factor. The design of the modified L3, which can be seen in **Figure 3**a through the map of Im[Ey], is obtained by cutting a clove out of the photonic crystal ($R = 7$) surrounding the cavity along one of the four $\Gamma - M$ diagonals occurring at 30.7°, through which the standard L3 typically drives the outgoing field. This allows to increase the QNM hybridization with leaky modes along this line where only two photonic crystal rows are present, while at the same time the photonic barrier on the other three $\Gamma - M$ diagonals allow to have $Q = 300$. Infact, as it can be deduced by Figure 3a, the imaginary part of the QNM of the engineered cavity redirects most of the losses in the cut area.

This is further confirmed by the asymmetric feature of the spatial profile of Im[Ey] along the horizontal black dashed line of Figure 3a reported in Figure 3b in red, together with the plotted value of $q = -\mathrm{Re[Ey]}/\mathrm{Im[Ey]}$ (blue dashed line); we see that inside the cavity the Fano parameter shows strong modulations that indicate the possibility of tracking non-Lorentzian lineshapes, even in points with relatively large LDOS. For this reason, two positions, highlighted by the green and purple squares in the plot of Figure 3b, were properly chosen to fall within the range of q values suggesting a Fano lineshape of the LDOS. The calculated LDOS are shown in Figure 3c (red spectra) and compared with the ones of the standard L3 with $R = 3$ (light blue spectra), where a similar Q-factor is found. The spectra were obtained by placing a dipole near the center of the cavity (x = −160 nm, yellow square) and a bit further from the center, but still inside the cavity (x = −390 nm, green square in Figure 3b). While the L3 in both positions still exhibits a quasi-Lorentzian lineshape (light blue spectrum), the modified L3 displays an LDOS with a Fano lineshape (red spectrum), respectively with $q = -3.8$ (upper panel) and $q = 4.4$ (lower panel), as predictable from the modulation of q shown in Figure 3b. These results demonstrate that the cut design of the L3 allows to increase $\tilde{\mathbf{E}}_C(\mathbf{r})/\tilde{\mathbf{E}}_B(\mathbf{r})$ inside the cavity area, and therefore to decrease the parameter q and to have a Fano lineshape inside the photonic cavity. Interestingly, by zooming the plot of q within a 100 nm range (Figure 3d), we can finely tune the position in which the LDOS can be calculated, in order to spot the transition from $q \approx -1$ to $q \approx 1$. The final calculations for three positions, highlighted respectively by a green (x = −141 nm), purple (x = −139 nm) and cyan (x = −137 nm) dot, are reported in Figure 3e in corresponding colors. The three LDOS, of smaller intensity with respect to the ones previously shown, clearly exhibit the typical shapes determined by $q \approx -1$, $q \approx 0$ and $q \approx 1$. It is worth noticing that in presence of a QNM in resonance with the emitter, the radiative rate could in

principle be decreased, with respect to the non-resonant value, as shown by the Lorentzian dip (that is $q \approx 0$) at x = -139 nm.

3. Conclusion

In conclusion, we have demonstrated the possibility to tailor the Fano spectral lineshapes of the photonic LDOS by controlling the spatial distribution of the leaky modes. The cavity engineering is driven by the predictions of an analytical model that is developed through a perturbation theory approach, in order to link non-Hermitian QNM normalization to the concept of interference. The model is based on the assumption that the QNM of a high-Q photonic cavity, after the introduction of a certain amount of losses, can be considered as a new QNM state that is the result of the hybridization between the initial high-Q state and a continuum state, determined by the leaky modes propagating out of the cavity. Indeed, from the general expression of the LDOS within non-Hermitian theories the LDOS of any QNM, even if it is of Lorentzian character at its center, is an asymmetric Fano inside the PhC in which it is embedded, with strong variations of the lineshape of the LDOS at the nanoscale.

However, in order to detect a Fano lineshape of the LDOS inside the cavity one should increase the contribution of the losses so high such that the Q-factor would be too low to be considered for any application and experimental demonstration. Inspired by this, we engineered a standard L3 that exhibits an LDOS with Fano lineshape inside the cavity itself, in positions where the LDOS is not too small. We believe that our results have shed light on the physical mechanisms underlying well known photonic features of the state-of-the-art devices for light confinement, i.e., PhC cavities, and might contribute for their practical exploitations in several fields such as quantum devices, optical switching, and sensing applications.

4. Experimental Section

Finite Element Method Simulations: The photonic cavities on slab were simulated with a finite-element complex eigensolver. Within the theoretical framework of QNMs, which were the solutions to the source-free Maxwell wave equation with a radiation boundary condition,[15,30,31] the photonic crystal resonances can be solved. The resulting eigenvalue problem admits solutions with complex eigenfrequencies $\tilde{\omega}_n = \omega_n - i\Gamma_n$. As a consequence of the radiation condition, the QNM fields diverge in the far-field, which invalidates common energy normalization approaches in Hermitian systems. This was circumvented through alternative normalization approaches that regularize the QNM behavior.[19] In this work the so-called perfectly matched layer (PML) normalization was used:

$$\iiint \left(\varepsilon \tilde{E}^2 - \mu_0 \tilde{H}^2\right) d^3r = 1 \tag{10}$$

where $\{\tilde{E}_n, \tilde{H}_n\}$ is the electromagnetic field of the QNM and the integral is calculated over the volume $V_T = V \cup V_{PML}$, i.e., the total volume that comprehends not only the volume surrounding the cavity (V), but also the volume occupied by the Perfectly Matching Layer (PML) used for the numerical implementation of the radiation condition.

Finite Difference Time Domain Simulations: FDTD simulations were employed to calculate the LDOS of the cavities. The spectra were obtained by calculating the flux of the Poynting vector exiting a closed squared box surrounding the dipole, which was y-polarized and spectrally centered ≈1250 and 200 nm broad.

For both types of simulations, the employed refractive index of Silicon was $n = 3.46$.

Conflict of Interest

The authors declare no conflict of interest.

Data Availability Statement

The data that support the findings of this study are available from the corresponding author upon reasonable request.

Keywords

fano profile, loss engineering, non-Hermitian theory, purcell effect, radiative rate

Received: July 3, 2023
Revised: October 12, 2023
Published online: October 31, 2023

[1] R. Soref, *APL Photonics* **2018**, *3*, 021101.
[2] J. R. Mejía-Salazar, O. N. Oliveira, *Chem. Rev.* **2018**, *118*, 10617.
[3] S. Pirandola, B. R. Bardhan, T. Gehring, C. Weedbrook, S. Lloyd, *Nat. Photonics* **2018**, *12*, 724.
[4] N. Granchi, M. Petruzzella, D. Balestri, A. Fiore, M. Gurioli, F. Intonti, *Opt. Express* **2019**, *27*, 37579.
[5] A. J. Shields, *Nat. Photonics* **2007**, *1*, 215.
[6] T. Ozawa, H. M. Price, A. Amo, N. Goldman, M. Hafezi, L. Lu, M. C. Rechtsman, D. Schuster, J. Simon, O. Zilberberg, I. Carusotto, *Rev. Modern Physics* **2019**, *91*, 015006,.
[7] E. M. Purcell, H. C. Torrey, R. V. Pound, *Phys. Rev.* **1946**, *69*, 37.
[8] Y. Akahane, T. Asano, B.-S. Song, S. Noda, *Nature* **2003**, *425*, 944.
[9] H. Sekoguchi, Y. Takahashi, T. Asano, S. Noda, *Opt. Express* **2014**, *22*, 916.
[10] N. Granchi, F. Intonti, M. Florescu, P. D. García, M. Gurioli, G. Arregui, *ACS Photonics* **2023**, *10*, 2808.
[11] S. Noda, M. Fujita, T. Asano, *Nat. Photonics* **2007**, *1*, 449.
[12] T. Amoah, M. Florescu, *Phys. Rev. B* **2015**, *91*, 020201.
[13] N. Granchi, M. Lodde, K. Stokkereit, R. Spalding, P. J. Van Veldhoven, R. Sapienza, A. Fiore, M. Gurioli, M. Florescu, F. Intonti, *Phys. Rev. B* **2023**, *107*, 064204.
[14] C. Sauvan, J. P. Hugonin, I. S. Maksymov, P. Lalanne, *Phys. Rev. Lett.* **2013**, *110*, 237401.
[15] P. Lalanne, W. Yan, K. Vynck, C. Sauvan, J.-P. Hugonin, *Laser Photonics Rev.* **2018**, *12*, 1700113.
[16] K. G. Cognée, W. Yan, F. La China, D. Balestri, F. Intonti, M. Gurioli, A. F. Koenderink, P. Lalanne, *Optica* **2019**, *6*, 269.
[17] D. Pellegrino, D. Balestri, N. Granchi, M. Ciardi, F. Intonti, F. Pagliano, A. Y. Silov, F. W. Otten, T. Wu, K. Vynck, P. Lalanne, A. Fiore, M. Gurioli, *Phys. Rev. Lett.* **2020**, *124*, 123902.
[18] N. Caselli, T. Wu, G. Arregui, N. Granchi, F. Intonti, P. Lalanne, M. Gurioli, *ACS Photonics* **2021**, *8*, 1258.
[19] P. T. Kristensen, R-C. Ge, S. Hughes, *Phys. Rev. A* **2015**, *92*, 053810.
[20] M. F. Limonov, M. V. Rybin, A. N. Poddubny, Y. S. Kivshar, *Nat. Photonics* **2017**, *11*, 543.
[21] L. Stern, M. Grajower, U. Levy, *Nat. Commun.* **2014**, *5*, 4865.
[22] N. Caselli, F. Intonti, F. La China, F. Biccari, F. Riboli, A. Gerardino, L. Li, E. H. Linfield, F. Pagliano, A. Fiore, M. Gurioli, *Nat. Commun.* **2018**, *9*, 396.

[23] C. Wu, A. B. Khanikaev, R. Adato, N. Arju, A. A. Yanik, H. Altug, G. Shvets, *Nat. Mater.* **2011**, *11*, 69.
[24] Y. Yu, W. Xue, E. Semenova, K. Yvind, J. Mork, *Nat. Photonics* **2016**, *11*, 81.
[25] U. Fano, *Phys. Rev.* **1961**, *124*, 1866.
[26] M. Galli, S. L. Portalupi, M. Belotti, L. C. Andreani, L. O'faolain, T. F. Krauss, *Appl. Phys. Lett.* **2009**, *94*, 071101.
[27] N. Caselli, F. Intonti, F. La China, F. Riboli, A. Gerardino, W. Bao, A. W. Bargioni, L. Li, E. H. Linfield, F. Pagliano, A. Fiore, M. Gurioli, *Light: Sci. Appl.* **2015**, *4*, e326.
[28] C. W. Hsu, B. Zhen, A. D. Stone, J. D. Joannopoulos, M. Soljačić, *Nat. Rev. Mater.* **2016**, *1*, 16048.
[29] F. Intonti, S. Vignolini, F. Riboli, A. Vinattieri, D. S. Wiersma, M. Colocci, L. Balet, C. Monat, C. Zinoni, L. H. Li, R. Houdré, M. Francardi, A. Gerardino, A. Fiore, M. Gurioli, *Phys. Rev. B* **2008**, *78*, 041401.
[30] P. T. Kristensen, K. Herrmann, F. Intravaia, K. Busch, *Adv. Opt. Photonics* **2020**, *12*, 612.
[31] COMSOL Multiphysics® v. 6.1. www.comsol.com COMSOL AB, Stockholm, Sweden (accessed: July 2023).